Memo for File
Updated December 2002

Small-Scale Self-Focusing Effects in Tapered Optical Beams

A. E. Siegman
Stanford University

Abstract

This memo presents a simple analysis of small-scale self focusing or filamentation effects in strongly diverging or converging optical beams ("tapered beams") propagating in nonlinear or saturable optical media. In contrast to the collimated beam case where the nonlinear perturbations can be modelled as uniformly spaced periodic ripples, the nonlinear phase and amplitude ripples in the tapered-beam case can be modeled as nonlinear Newton's rings or Fresnel zone plates. These perturbations, although they preserve their shape with distance, do not grow exponentially with distance as in the collimated beam case because they lack the Talbot interaction that is necessary for exponential growth. Instead they tend to grow either logarithmically or as a power of z with distance.

1. Introduction

Small-scale self focusing in optical Kerr media is a well-understood process in which periodic small-amplitude amplitude or phase ripples on the transverse profile of a collimated optical beam grow exponentially with distance as the beam passes through a nonlinear medium. After sufficiently large growth these ripples may evolve into intense "filaments" with peak intensities sufficient to damage the material in which they propagate.

The basic mechanism involved in small-scale self focusing was first analyzed in two classic papers by Bespalov and Talanov [1,2], followed in subsequent years by many further theoretical and experimental discussions [3–8]. These early studies of small-scale self focusing provided experimental confirmation for the optical Kerr effect and served as an interesting complement to the companion process of large-scale or whole-beam self focusing [9]. In subsequent years understanding of this effect has helped to explain and control beam-quality degradation and optical damage mechanisms in high-power laser amplifiers [10,11], and in recent years extensions of these ideas have helped to understand and control unwanted filamentation effects in wide-stripe semiconductor lasers [12–16].

Self-focusing and filamentation effects can also be observed to some extent in tapered (diverging or converging) optical beams [17,18], although with more difficulty. Clean and well-characterized self-focusing behavior involving a self-preserving transverse beam profile does not seem to have been observed in tapered beams, and no simple analytical model for this case seems to have yet been developed. Theoretical studies of the tapered-beam case have generally been limited to numerical simulations [19–21].

In this note I present a simple physical model and the resulting analytical solutions for small-scale self focusing of strongly divergent or convergent optical beams propagating in either optical Kerr media (nonlinear phase modulation) or in saturable gain or loss media (nonlinear amplitude modulation). In this analysis the shape-preserving phase and amplitude patterns that may occur in tapered beams are identified as nonlinear Newton's rings or Fresnel zone plates. An analysis closely analogous to the original Bespalov and Talanov formulation then shows that these patterns, although persisting in form with distance, will in general not grow exponentially with distance as they do in the collimated beam case. The phase portion of these perturbations does grow with distance, but at most either logarithmically or as a power of z. One implication of this is that filamentation effects in tapered beams, including tapered amplifiers, should (fortunately) be significantly less intrusive and easier to control than in the comparable collimated beam case. There may also be implications in this analysis for the formation of nonlinear coherent optical beam patterns in tapered beams

2. Collimated Beam Analysis

It may be useful to review the elementary analysis of these phenomena for the collimated optical beam case before tackling the tapered-beam case. We assume a medium having an optical Kerr effect and potentially a (weakly) saturable gain coefficient. The complex propagation constant $\tilde{k}$ for waves in such a medium can then be approximated by

$$\tilde{k} = [k_0 - k_2\, I] + j[g_0 - g_2\, I] \tag{1}$$

where $I = I(x,y,z)$ is the local intensity (power per unit area) in the medium. The nonlinear paraxial wave equation for the complex phasor wave amplitude $\tilde{u}(x,y,z)$ of a beam propagating in the z direction through such a medium can then be written as

$$\left[\nabla^2_{xy} - 2jk_0 \frac{\partial}{\partial z} + 2jk_0 g_0 + 2k_0(k_2 - jg_2)I(x,y,z)\right] \tilde{u}(x,y,z) = 0\ . \tag{2}$$

In the collimated case the basic approach is to assume that the optical beam consists of a uniform collimated primary plane wave traveling in the z direction with amplitude u_0 at $z = 0$, plus two weak secondary waves with small fractional amplitudes $\tilde{c}_1(z)$ and $\tilde{c}_2(z)$ traveling at small angles $\pm\theta$ to the main beam. The complex beam amplitude profile can then be written (limiting the analysis to one transverse direction) as

$$\tilde{u}(x,z) = u_0\, e^{g(z) - j\phi(z)} \times [1 + \tilde{c}_1(z)e^{j\kappa x} + \tilde{c}_2(z)e^{-j\kappa x}] \tag{3}$$

where $\kappa = k_0 \sin\theta$ is a transverse k vector. The exponential factor $g(z)$ allows for the overall gain of the beam amplitude with distance due to any gain coefficient g_0 in the medium, while the phase shift $\phi(z)$ allows for a change in overall propagation constant beam due to the optical Kerr effect. Putting this expansion into the nonlinear wave equation and dropping higher-order terms than leads to the coupled equations for $\tilde{c}_1$ and $\tilde{c}_2$

$$\frac{d\tilde{c}_1(z)}{dz} = j\left[\frac{\kappa^2}{2k_0} - (k_2 - jg_2)\, u_0^2 e^{2g(z)}\right] \tilde{c}_1(z) - j\left[(k_2 - jg_2)\, u_0^2 e^{2g(z)}\right] \tilde{c}_2^\star(z) \tag{4}$$

and

$$\frac{d\tilde{c}_2^\star(z)}{dz} = -j\left[\frac{\kappa^2}{2k_0} - (k_2 - jg_2)\, u_0^2 e^{2g(z)}\right] \tilde{c}_2^\star(z) + j\left[(k_2 - jg_2)\, u_0^2 e^{2g(z)}\right] \tilde{c}_1(z) \tag{5}$$

Setting up the analysis in this fashion provides physical insight, and in particular emphasizes that the basic mechanism for the exponential growth of small-scale self focusing is a combination of Talbot phase shifts (the $\kappa^2/2k_0$ terms) plus nonlinear coupling between the two weak secondary waves facilitated by the strong primary wave (the k_2 and g_2 terms). The Talbot phase shift terms show how the propagation of each tilted plane wave differs from axial propagation with wave vector k_0. The additional terms involving $k_2 - j g_2$ arise because interference between the primary wave and either of the weak secondary waves leads to the formation of periodic interference fringes and thus to nonlinearly induced phase or amplitude gratings which have transverse wave vector $\pm\kappa$ and strength proportional to the primary wave amplitude $u_0\, e^{g(z)}$. These gratings then diffract energy from the primary wave into both of the secondary waves, leading to the nonlinear coupling terms

These two coupled equations can be readily solved as they stand. The analysis becomes somewhat simpler algebraically however if we instead expand the transverse perturbations in cosine and sine form, with complex-valued cosine and sine amplitudes $\tilde{c}(z)$ and $\tilde{s}(z)$, in the form

$$\tilde{u}(x,z) = u_0\, \exp[g(z) - j\phi(z)] \times [1 + \tilde{c}(z) \cos \kappa x + \tilde{s}(z) \sin \kappa x] \tag{6}$$

Since the cosine and sine terms are the same except for a lateral translation, they both obey the same (uncoupled) first-order equation and only one of them, let's say the cosine term, needs to be considered. Putting this ansatz into the nonlinear wave equation, separating out the constant and periodic transverse terms in x, and retaining only first-order terms in the small cosine amplitude $\tilde{c}(z)$ leads first of all to a pair of zero-order equations for the growth of the overall amplitude and phase of these waves, namely

$$\frac{dg(z)}{dz} = g_0 - g_2\, u_0^2\, \exp[2g(z)] \tag{7}$$

and

$$\frac{d\phi(z)}{dz} = k_2\, u_0^2\, \exp[2g(z)]\ . \tag{8}$$

The first of these equations obviously describes the amplitude growth with distance due to the gain coefficient g_0 with first-order gain saturation taken into account, while the second equation describes the overall phase shift $\phi(z)$ due to the optical Kerr effect produced by the primary beam amplitude.

Of more importance is the equation describing the first-order growth of the cosine ripple coefficient $\tilde{c}(z)$ with distance, which is given by

$$\frac{d\tilde{c}(z)}{dz} = j\,\frac{\kappa^2}{2k_0}\,\tilde{c}(z) - j(k_2 - jg_2)u_0^2\, e^{2g(z)}[\tilde{c}(z) + \tilde{c}^*(z)] \tag{9}$$

At this point it is useful to separate the coefficient c into real and imaginary parts, i.e., $\tilde{c}(z) \equiv c_r(z) + j\, c_i(z)$. Writing the intensity profile across the beam as

$$I(x,z) = |\tilde{u}(x,z)|^2 \simeq u_0^2\, e^{2g(z)}[1 + 2c_r(z)\cos\kappa x] \tag{10}$$

then makes clear that the real part ofthe cosine amplitude, or $c_r(z)$, represents a periodic amplitude ripple on the beam, while the imaginary part $c_i(z)$ represents to first order only a periodic phase ripple on the beam wavefront. The growth equation for $\tilde{c}(z)$ can then be separated into

$$\frac{dc_r}{dz} = -\left(\frac{\kappa^2}{2k_0}\right) c_i - 2g_2 u_0^2 c_r \tag{11}$$

and

$$\frac{dc_i}{dz} = \left(\frac{\kappa^2}{2k_0} - 2k_2 u_0^2\right) \; . \tag{12}$$

These results say that in the absence of any nonlinearity, i.e., if $k_2 = g_2 = 0$, the coefficients $c_r(z)$ and $c_i(z)$ both oscillate (or rotate in phase) with distance as a result of the axial propagation factor $\kappa^2/2k_0$. This rotation is essentially the well-known Talbot phase shift factor.

If one then adds an optical Kerr coefficient k_2 into these equations, but leaves out any saturable gain coefficient $g_2 = 0$, both $c_n(z)$ and $c_i(z)$ acquire an exponential growth with distance of the form $\tilde{c}(z) \propto \exp[\pm\gamma z]$ where the growth coefficient γ is given by

$$\gamma^2 = \left(\frac{\kappa^2}{2k_0}\right)\left[2k_2 u_0^2 - \left(\frac{\kappa^2}{2k_0}\right)\right] \; . \tag{13)(9}$$

This growth rate has a maximum value $\gamma_{\max} = k_2 u_0^2$ for ripples with a spatial period given by $\kappa_{\max} = \sqrt{2k_0 k_2 u_0^2}$.

One can also find from the preceding equations that a saturable gain or loss medium, that is, a medium characterized by a finite value for g_2 but with $k_2 = 0$, does not lead to this kind of exponential ripple growth. For a saturable gain medium, if we again ignore the overall $\exp[2g(z)]$ amplification, the roots for the ripple growth become

$$\gamma = -\, g_2 u_0^2 \pm \sqrt{(g_2 u_0^2)^2 - (\kappa^2/2k_0)^2} \; , \tag{14}$$

so that both roots represent attenuation with distance rather than growth.

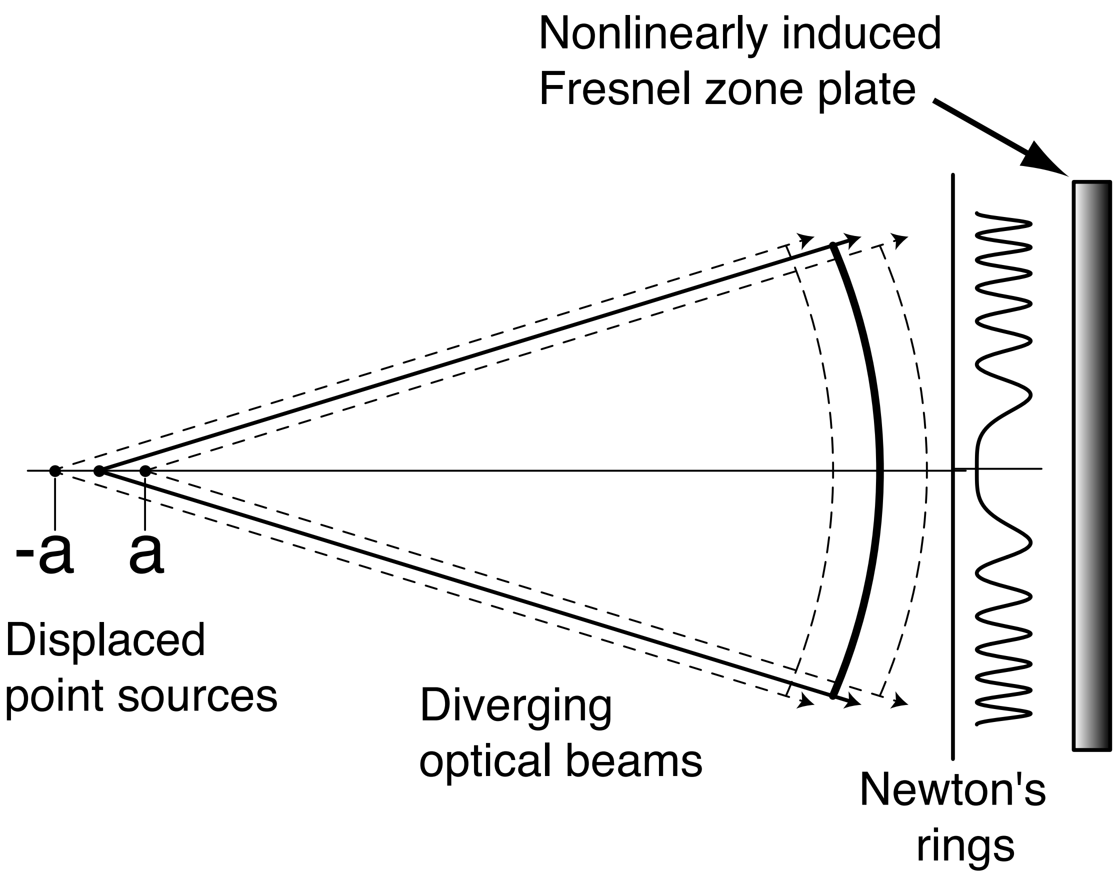

Figure 1. The diverging spherical wave model used in the analysis, and the Fresnel zone plate or Newton's rings pattern produced by interference between the primary spherical wave and either of the weaker secondary waves.

3. Tapered beam analysis

We now develop a similar analysis for the tapered beam case. The crucial step in this approach is to replace the primary and secondary *plane waves* in the collimated model by primary and secondary *spherical* or *cylindrical waves* that diverge from a source point or focus located on axis at $z = 0$, plus two additional axially displaced source points which are located on the propagation axis at distances $z = \pm a$ behind and in front of the primary wave focal point, as shown in Fig. 1.

The cylindrical-wave and spherical-wave cases can then be treated in a single formalism if we write the complex amplitude of the tapered beam in a form analogous to the plane-wave expansion, that is, as

$$\begin{aligned}\tilde{u}(x,z) = \; & u_0\, e^{g(z)-j\phi(z)} \left[\frac{1}{z^{n/2}} \exp\left(-j\frac{kx^2}{2z}\right) \right. \\ & + \quad \tilde{c}_1(z) \frac{1}{(z+a)^{n/2}} \exp\left(-j\frac{kx^2}{2(z+a)}\right) \\ & \left. + \quad \tilde{c}_2(z) \frac{1}{(z-a)^{n/2}} \exp\left(-j\frac{kx^2}{2(z-a)}\right)\right] .\end{aligned} \tag{15}$$

where the index n again has the value $n = 1$ for the cylindrical wave case or $n = 2$ for the spherical wave case, and with x being replaced by the transverse radial coordinate r in the spherical case. The first exponential factor inside the rectangular brackets is of course the primary wave diverging from (or converging to) $z = 0$, while the second and third exponential factors are the secondary waves diverging from $z = \pm a$. Suppose we now consider these waves at distances z far enough away from their source points so that we can make the primary approximation of this analysis, namely $|z| \gg a$. The beam profile expression above can then be expanded to first order in powers of a/z in the form

$$\tilde{u}(x,z) \simeq \frac{u_0\, \exp[g(z) - j\phi(z) - jkx^2/2z]}{z^{n/2}} \left[1 + \tilde{c}(z)\, \cos\frac{k\,ax^2}{2z^2} + \tilde{s}(z) \sin\, \frac{k\,ax^2}{2z^2} \right] \tag{16}$$

The physical picture in this case is that the weak secondary waves coming from $z = \pm a$ interfere with the primary spherical wave coming from $z = 0$ to produce in essence a set of Newton's rings having a transverse or radial variation of the form $\cos(k\,ax^2/2z^2)$ or $\sin(k\,ax^2/2z^2)$, as also illustrated in Fig. 1. These rings diverge (or converge) in the form of cones that have fixed angular positions within the overall tapered beam, at least for $z \gg a$.

These rings, however, will also act through the nonlinear properties of the medium to produce in effect continuous Fresnel zone plates or gratings at each transverse plane of the medium. These zone plates will be of phase or amplitude character depending on the optical Kerr and saturable gain coefficients k_2 and g_2, respectively. In either case, however, these Fresnel zone plates will have exactly the right form to diffract energy from the primary spherical wave into the weak secondary waves originating from $z = \pm a$. This coupling back into the same secondary spherical waves is the direct analog in the tapered case to the diffraction coupling of the weak secondary waves at $\pm\theta$ into each other in the collimated beam case.

The analytical and physical consequences of these diffraction effects are, however, quite different in the tapered beam case than in the collimated beam case. If the wave expansion above is substituted into the nonlinear wave equation using the same small-signal approximations as in the collimated beam case, the constant or primary-wave terms again lead to a pair of overall gain and phase shift equations, namely

$$\frac{dg(z)}{dz} = g_0 - \frac{g_2 u_0^2}{z^n}\, e^{2g(z)} \tag{17}$$

and

$$\frac{d\phi(z)}{dz} = \frac{k_2 u_0^2}{z^n}\, e^{2g(z)} \tag{18}$$

which are essentially the same as in the collimated beam case, except that the tapered beam intensity $I(x,z)$ now has a $1/z^n$ variation due to the beam divergence or convergence. The growth equation for the cosinusoidal beam profile coefficient $\tilde{c}(z)$, however, takes on the modified form

$$\frac{d\tilde{c}(z)}{dz} = -j(k_2 - jg_2)\,\frac{u_0^2\, e^{2g(z)}}{z^n}\,[\tilde{c}(z) + \tilde{c}^*(z)]\ . \tag{19}$$

This equation is significantly different from the collimated beam result. In particular, the Talbot term $\kappa^2/2k_0$ appearing in the collimated beam equations is no longer present in the tapered beam case, at least for $z \gg a$, so that $d\tilde{c}/dz = d\tilde{s}/dz \simeq 0$ in the absence of any nonlinear effects. There is no analog to the Talbott effect in the tapered beam case.

4. Tapered Beam Results

Suppose we again write the ripple profile coefficient as $\tilde{c}(z) \equiv c_r(z) + j(c_i(z)$ with c_r representing an amplitude or intensity ripple and c_i to first order representing only a phase ripple in the beam profile. We can then consider the solutions to the above equations for the four limiting cases of cylindrical or spherical waves ($n = 1$ or $n = 2$) and pure index or pure gain saturation ($g_2 = 0$ or $k_2 = 0$). The analytic solutions for these four ideal limiting cases, assuming for simplicity that any overall gain in the medium is small enough so that $2g(z) \ll 1$, are then:

(a) Cylindrical wave $(n = 1)$ *and pure optical Kerr effect* $(g_2 = 0)$

The equations in this case separate into

$$\frac{dc_r(z)}{dz} = 0 \qquad \text{and} \qquad \frac{dc_i(z)}{dz} \simeq -\,\frac{2k_2 u_0^2}{z}\, c_r(z) \tag{20}$$

with analytic solutions

$$c_r(z) = c_{r0} \quad \text{and} \quad c_i(z) = c_{i0} - [2k_2 u_0^2 \log(z/z_0)]\, c_r \tag{21}$$

where c_{r0} and c_{i0} are initial amplitudes at a starting plane $z = z_0$. The small-signal growth of the Fresnel ripples with distance in this case is only proportional to $\log(z/z_0)$ and of more importance it occurs only in the coefficient $c_i(z)$ which is the phase-ripple portion of the profile. The intensity perturbations on the beam do not grow at all with distance, at least not in a first-order approximation.

(b) Cylindrical wave $(n = 1)$ *and pure gain saturation* $(k_2 = 0)$

The approximate equations are now

$$\frac{dc_r(z)}{dz} \simeq -\,\frac{2g_2 u_0^2}{z}\, c_r(z) \qquad \text{and} \qquad \frac{dc_i(z)}{dz} \simeq 0 \tag{22}$$

with solutions

$$c_r(z) = \left(\frac{z_0}{z}\right)^{2g_2 u_0^2} c_{r0} \quad \text{and} \quad c_i(z) = c_{i0}\ . \tag{23}$$

In this case any initial intensity ripples die out with distance, while any initial phase ripples remain unchanged with distance.

(c) Spherical wave $(n = 2)$ *and pure optical Kerr effect* $(g_2 = 0)$

The equations in this case are the same as above except that $1/z$ is replaced by $1/z^2$. The solutions then become

$$c_r(z) = c_{r0} \quad \text{and} \quad c_i(z) = c_{i0} - 2k^2 u_0^2 \left(\frac{1}{z_0} - \frac{1}{z}\right) c_{r0}\ . \tag{24}$$

Again the intensity ripples remain constant while the phase ripples can grow with distance, but only to a certain limited value which depends on the input intensity. In essence, as the beam spreads the intensity drops sufficiently rapidly so that even the phase ripples cease to grow.

(d) Spherical wave ($n = 2$) and pure gain saturation ($k_2 = 0$)

Finally, replacing $1/z$ with $1/z^2$ in the gain saturation case gives the solutions

$$c_r(z) = c_{r0} \exp\left[-2k_2 u_0^2 \left(\frac{1}{z_0} - \frac{1}{z}\right)\right] \quad \text{and} \quad c_i(z) = c_{i0} \ . \tag{25}$$

Again the intensity ripples decrease with distance, while the phase ripples remain unchanged.

5. The Strongly Tapered Approximation

In closing, it is important to understand the physical conditions under which the "strongly tapered" approximation $z \gg a$ used in this analysis can be valid. This can be approached in two more or less equivalent fashions. As a first approach let us consider a tapered or conical beam with a uniform intensity profile extending over a half-angle $\pm\theta_1$. The outer radius of this beam at distance z will then be given by $x_1 \simeq \theta_1 z$ and the number of Fresnel rings within this radius, call it N_R, will be given by

$$\cos\left(\frac{\pi a x_1^2}{z^2 \lambda}\right) \simeq \cos\left(N_R \cdot 2\pi\right) \qquad \text{or} \qquad N_R \simeq \frac{a x_1^2}{2 z^2 \lambda} \simeq \left(\frac{a}{2\lambda}\right) \theta_1^2 \ . \tag{26}$$

For the analysis presented in this paper to be meaningful the Fresnel zone plate should have at least at modest number of rings, perhaps $N_R \simeq 4$ or greater. In a typical tapered beam where the divergence half-angle θ_1 may be a fraction of radian, this obviously requires that the longitudinal offset of the secondary foci have a value $a \gg \lambda$, and then in turn that the observation region satisfy $|a| \gg a$.

As a more specific example let us suppose the primary beam is a TEM_{00} beam with a transverse intensity profile $I(x, z) = I_0 \exp[-2x^2/w^2(z)]$ where the gaussian spot size $w(z)$ is given in terms of the Rayleigh range $z_R = \pi w_0^2/\lambda$ by $w^2(z) = w_0^2[1+(z/z_R)^2] \simeq (\lambda/\pi z_R) z^2$. The number of Fresnel rings within central peak of this gaussian profile, let us say out to a radius $x = w/2$, will then be given by

$$N_R = \frac{1}{8\pi} \frac{a}{z_R} \tag{27}$$

The requirement to have some reasonable number of Fresnel rings within the central portion of the TEM_{00} beam is then evidently $a \gg z_r$ and again $|z| \gg a$.

6. Conclusions

The primary conclusions from these results appear to be that:

1) The small-scale self focusing or filamentation effects are very different for tapered as compared to collimated beams. In particular the zone-plate intensity ripples on tapered beams do not seem to show exponential small-signal growth under any circumstances, while the phase ripples only show weak and limited growth.

3) This behavior appears to be related analytically to the loss of the Talbot phase shift term, an effect which in the collimated beam case periodically converts phase ripples into amplitude ripples and vice versa, thereby making possible the exponential growth of the phase-grating-induced ripples.

2) Self-focusing is thus a very ineffectual process for strongly tapered beams in optical Kerr media or other nonlinear index materials as compared to small-scale self focusing in collimated beams.

These conclusions are of course in good agreement with previous experimental and numerical results and with physical intuition. It will of course be interesting to see if more detailed numerical calculations on a nonlinear tapered beam model can verify the simple analytical results presented in this paper.

Acknowledgements

The author expresses appreciation for support for this work from the Air Force Office of Scientific Research.

REFERENCES

1. V. I. Bespalov and V. I. Talanov, "Filamentary structure of light beams in nonlinear liquids," *Sov. Phys. JETP Lett.* **3**, 307–310 (15 June 1966).
2. V. I. Talanov, "Focusing of light in cubic media," *Sov. Phys. JETP Lett.* **11**, 199–201 (1970).
3. Campillo, Shapiro and B. R. Suydam, "Periodic breakup of optical beams due to self-focusing," *Appl. Phys. Lett.* **23**, 628 (1 December 1973).
4. Campillo, Shapiro and B. R. Suydam, "Relationship of self-focusing to spatial instability modes," *Appl. Phys. Lett.* **24**, 178–180 (15 February 1974).

5. E. S. Bliss, D. R. Speck, J. F. Holtzrichter, J. H. Erkkila and A. J. Glass, "Propagation of a high-intensity laser pulse with small-scale intensity modulation," *Appl. Phys. Lett.* **25**, 448–450 (15 October 1974).
6. B. R. Suydam, "Self-focusing of very powerful laser beams II," *IEEE J. Quantum Electron.* **QE–10**, 837–843 (November 1974).
7. S. C. Abbi and N. C. Kothari, "Theory of filament formation in self-focusing media," *Phys. Rev. Lett.* **43**, 1929–32 (24 December 1979).
8. S. C. Abbi and N. C. Kothari, "Growth of Gaussian instabilities in Gaussian laser beams," *J. Appl. Phys.* **51**, 1385–1387 (March 1980).
9. S. A. Ahkmanov, R. V. Khokhlov and A. P. Sukhorukov, "Self-focusing, self-defocusing and self-modulation of laser beams," in *Laser Handbook* (North-Holland, 1972) pp. 1151–1228.
10. B. R. Suydam, "Effect of refractive-index nonlinearity on the optical quality of high-power laser beams," *IEEE J. Quantum Electron.* **QE–11**, 225–230 (June 1975).
11. D. C. Brown *The Physics of high Peak Power Nd:Glass Laser Systems* (Springer-Verlag, Heidelberg, 1980).
12. A. H. Paxton and G. C. Dente, "Filament formation in semiconductor laser gain regions," *J. Appl. Phys.* **70**, 2921–2925 (15 September 1991).
13. R. J. Lang, D. Mehuys, A. Hardy, K. M. Dzurko and D. F. Welch, "Spatial evolution of filaments in broad area diode laser amplifiers," *Appl. Phys. Lett.* **62**, 1209–1211 (15 March 1993).
14. R. J. Lang, D. Mehuys, D. F. Welch and L. Goldberg, "Spontaneous filamentation in broad-area diode laser amplifiers," *IEEE J. Quantum Electron.* **QE–30**, 685–694 (March 1994).
15. O. Hess, S. W. Koch and J. V. Moloney, "Filamentation and beam propagation in broad-area semiconductor lasers," *IEEE J. Quantum Electron.* **QE–31**, 35–43 (January 1995).
16. J. R. Marciante and G. P. Agrawal, "Nonlinear mechanisms of filamentation in broad-area semiconductor lasers," *IEEE J. Quantum Electron.* **QE–32**, 590–596 (April 1996).

17. A. H. Paxton, “Formation of filaments in expanding beams in semiconductor amplifiers,” in *Laser Resonators and Coherent Optics: Modeling, Technology, and Applications: Proc. SPIE 1868*, Los Angeles, California (January 1993).

18. L. Goldberg, M. R. Surette and D. Mehuys, “Filament formation in a tapered GaAlAs optical amplifier,” *Appl. Phys. Lett.* **62**, 2304 (10 May 1993).

19. R. J. Lang, A. Hardy, R. Parke, D. Mehuys, S. O’Brien, J. Major and D. Welch, “Numerical analysis of flared semiconductor laser amplifiers,” *IEEE J. Quantum Electron.* **QE–29**, 2044–2051 (June 1993).

20. S. Ramanujan and H. G. Winful, “Spontaneous emission induced filamentation in flared amplifiers,” *IEEE J. Quantum Electron.* **QE–32**, 784–789 (May 1996).

21. G. Levy and A. A. Hardy, “Chaotic effects in flared lasers: a numerical analysis,” *IEEE J. Quantum Electron.* **QE–33**, 26-32 (January 1997).